International Journal of Materials and Chemistry 2017, 7(2): 25-35
DOI: 10.5923/j.ijmc.20170702.02

Comparative Sorption Studies of Dyes and Metal Ions by Ni/Al-Layered Double Hydroxide

Ayawei Nimibofa*, Ebelegi N. Augustus, Wankasi, Donbebe

Department of Chemical Sciences, Niger Delta University, Wilberforce Island, Nigeria

Abstract Anionic clay Ni/Al Layered double hydroxide (Ni/Al-LDHs) with M^{2+}:M^{3+} of (4:1, 3:1, 2:1 and 1:1) ratios were synthesized by co-precipitation method from nitrate salt solutions. The synthesized LDHs were characterized by thermo-gravimetric analysis, Fourier transform infrared spectroscopy, X-Ray Diffraction, Energy Dispersive Spectroscopy/Scanning Electronic Microscopy and Thermogravimetric spectroscopy. The effects of contact time, temperature and initial concentrations on the adsorption of lead, copper, congo red and methylene blue were investigated to optimize the conditions for maximum adsorption. The experimental data from the batch adsorption studies were subjected to equilibrium studies using Langmuir, Freundlich, Temkin and Dubinin-Kaganer-Radushkevic isotherms and found to be consistent with physical adsorption. The results from the thermodynamic studies also indicated, that the adosprtion of dyes was endothermic while that of metal ions was exothermic.

Keywords Kinetics, Adsorption, Thermodynamics, Methylene blue, Lead, Congo red, Copper, Equilibrium

1. Introduction

The industrial revolution of the past four decades has also caused serious pollution problems to mankind such that our continued existence on earth is threatened. Several pollutants such as dyes and heavy metals are continually released to aquifers and other water bodies all over the world. This has lead Governments and Scientists all over to scramble for solutions with a view to saving mother earth. Major sources of pollutants such as dyes and heavy metals includes petrochemical industries, textiles industries, mines, etc [1, 2]. They are known to cause serious health effect at high concentrations to humans [3-6]. Thus the need to removing them from water sources becomes imperative.

Several methods have been developed for the removal of dyes and heavy metals from wastewaters. These include physiochemical, chemical and biological methods such as coagulation and flocculation [7], ozonation [8], electrochemical methods [9], fungal decolonization [10] and adsorption [11-14]. Amongst the techniques mentioned, adsorption is the method of choice because of its ease of operation and design.

Recently, Layered double hydroxides (LDH), also known as hydrotalcites, have been widely used as adsorbent for various applications due to their unique anion exchange capability. In addition, the spent adsorbent can be easily regenerated and its adsorption capacities are comparable with the fresh LDH adsorbents [15-17]. In general, LDH consists of positively charged metal hydroxide sheets with anions located between the layers to compensate the positive layer charges. The composition of LDH is generally represented by the following equation [17-20]:

$$\left[M^{2+}_{1-x}M^{3+}_{x}(OH)_2\right]x^{+}A^{n-}_{x/n}mH_2O$$

where M^{2+} represents divalent cations $\left(Ca^{2+}, Mg^{2+}, Zn^{2+}, Co^{2+}, Ni^{2+}, Cu^{2+}, Mn^{2+}\right), M^{3+}$ represents trivalent cations $\left(Al^{3+}, Cr^{3+}, Fe^{3+}, Co^{3+}, Mn^{3+}\right)$ represents inorganic or organic anions $(Ci^{3+}, NO_3^-, CIO_{/1}^-, CO^{2-}_3, SO^{2-}_{/1})$ m is the number of interlayer water and $X(= M^{2+}/(M^{2+} + M^{3+})$ is the layer charge density of LDH. Due to their exchange capacity multiple uses have been adduced these hydrotalcites [21-23].

This work was aimed at successfully synthesizing Ni/Al-CO_3, and hydrotalcite in the laboratory for the adsorption of dyes and heavy metals in wastewater, understanding that access to clean water is still a fundamental problem in the world.

2. Materials and Methods

Carbonate form of Ni-Al LDH

A 50ml aqueous solution containing 0.3M $Ni(NO_3)_2.6H_2O$ and 0.1M Al $(NO_3)_3.6H_2O$ with Ni/Al ratio 4:1, was added drop wise into a 50 ml mixed solution of (NaOH (2M) and Na_2CO_3 (1M) with vigorous stirring and maintaining a pH of greater than 10 at room temperature. After complete addition,

* Corresponding author:
ayawei4acad@gmail.com (Ayawei Nimibofa)
Published online at http://journal.sapub.org/ijmc

the slurry formed was aged at 60℃ for 18 and 24 hrs respectively. The products were centrifuged at 5000 rpm for 5 minutes, with distilled water three to four times and dried by freeze drying. The same procedure was followed to synthesize LDHs with Ni^{2+}:Al^{3+} ratios of 3:1, 2:1 and 1:1 respectively.

Characterization of the LDHs

The X-ray powder diffraction pattern of synthesized LDH was taken with a Scintag diffractometer operated at 35 kV voltage and 30 mA current using CuKα radiation. A step scan of 5° /min was used in the continuous method in a range of 5-40° 2θ.

SEM measurements were performed using Hitachi S4100 with electron beam energy of 25 keV and Hitachi SU-70 scanning electron microscope (SEM) coupled with energy dispersive spectroscopy (EDS). LDHs for measurements were dispersed in ethanol or water using ultrasound and were later placed on the H-terminated silica on the holder.

FT-IR absorption spectra of the samples were recorded in a Perkin-Elmer FT-IR spectrometer (Model-FT-1730). The powdered samples completely dried were ground with KBr in 1:20 sample ratio and pressed to form a disc. This disc was placed in the sample holder of the FT-IR for the IR determination. Sixty four (64) spectra (recorded with a nominal resolution of 4 cm^{-1}) were accumulated and averaged to improve the signal-to- noise ratio.

Preparation of Metal Solutions/Dyes Solutions

A stock solution of 1000mgl^{-1} was prepared by dissolving 1.127g Methylene blue in 1000ml distilled water. This gave the Methylene blue stock. The experimental solution was prepared by diluting the stock solution with distilled water to between 20 - 40mgl^{-1}. The concentration of MB was determined at 630nm by the UV – visible spectrophotometer.

The analytical grade Congo red dye supplied by Labchem Laboratory was used as received. Stock solution of the dye was prepared by dissolving 1g solute in 1000ml volumetric flasks to make 1000 mg/L of the dye solution. Model and working calibration standards were prepared by serial dilution of the stock solution to concentrations of 20, 30 and 40mgl^{-1}.

Stock solution of lead nitrate [$Pb(NO_3)_2$] was prepared by dissolving 3.312g in 100ml of de-ionized water to obtain concentrations of 0.13 g/L Pb, 0.25 g/L Pb and 0.38 g/L Pb for the adsorption studies.

Working solutions of 0.08 g/L Cu, 0.12 g/L Cu and 0.16 g/L Cu were prepared by dissolving 1.6g of copper sulphate ($CuSO_4$) in 100ml of de-ionized water for the various batch adsorption studies.

Batch Adsorption Procedure

A 0.2g each of the powdered sample was collected and weighed out using an electronic weighing balance; the weighed sample was placed in three (3) pre-cleaned tubes. 10ml of the dye solutions (MB and CR) with standard concentrations of 20mg/L made from the stock solution in 3.6 above was added to each test tube containing the weighed sample and equilibrated by shaking (agitation) for 1 hour at temperatures of 40°C, 60°C and 80°C respectively using a compenstant Gallenhamp water bath. This was immediately centrifuged at 2500rpm for 5 minutes and then decanted. The supernatant were stored for dye UV-analysis. The same procedure was used for the analysis of metal ions (Pb^{2+} and Cu^{2+}) from standard spectroscopic grade lead nitrate ($Pb(NO_3)_2$ and copper sulphate ($CuSO_4$) using initial concentrations of 0.38g/L and 0.16g/L respectively.

A 0.2g each of the powdered sample of LDH was weighed out using an electronic weighing balance and the weighed sample was placed in three (3) pre-cleaned test tubes. 10ml of each metal ion solution with standard concentrations for (0.13, 0.25, 0.38) g/L and (0.08, 0.12, 0.16) g/L for Cu^{2+} which were made from spectroscopic grade standards of lead nitrate ($Pb(NO_3)_2$) and copper sulphate ($CuSO_4$) were added to each test tube containing the weighed sample and equilibrated by shaking (agitation) for 1 hour and then centrifuged at 2500rpm for 5 minutes and decanted. The supernatants were stored for the metal ion (Pb^{2+} and Cu^{2+}) analysis. Concentrations of (20, 30 and 40) mg/L were used for methylene blue (MB) and congo red (CR) respectively. The supernatants were then stored for UV-analysis.

A 0.2g each of the powdered sample of LDHs was weighed using an electronic weighing balance and placed in three (3) pre-cleaned test tubes. 10ml of the metal ion (Pb^{2+} and Cu^{2+}) solutions with concentration of 0.35g/L and 0.16g/L made from spectroscopic grade standard of lead nitrate ($Pb(NO_3)$ and copper sulphate ($CuSO_4$) were added to each test tube containing the weighed sample and equilibrated by shaking (agitation) for each time intervals of 10, 20 and 30 minutes respectively. The sample suspensions were centrifuged for 5 minutes at 2500rpm and decanted and the supernatants stored for metal ion (Pb^{2+} and Cu^{2+}) analysis. For the time studies of dyes (MB and CR), initial concentration of 20mg/L were used for the time differential studies and supernatants store and used for UV-analysis.

Metal Analysis

The concentration of CR and MB in the experimental solutions were determined from the calibration curve prepared by measuring the absorbance of different known concentrations of CR and MB solutions at wavelengths of 497 nm and 680nm respectively using a UV-vis spectrophotometer (Shimadzu, Kyoto, Japan).

The metal analysis (Pb^{2+} and Cu^{2+}) was performed by AAS using a buck scientific atomic absorption Spectrophotometer 200A (AAS).

Data Analysis

The various experimental data were subjected to equilibrium, thermodynamics and kinetic analysis for proper interpretation of adsorption processes.

Isotherms Equilibrium Analysis

The interpretation of adsorption capacity (q_e) and the sorption efficiency (R%) was done using equations 1 and 2

below:

$$q_e = \frac{C_i - C_e}{m} \quad (1)$$

$$R\% = \frac{C_i - C_e}{C_e}\, x\, 100 \quad (2)$$

where C_i and C_e are, respectively, the initial and equilibrium concentrations of metal ions/dyes in solutions (mmol/L) and m is the mass of the layered double hydroxides dosage (g).

The data for the uptake of dyes and metals at different temperatures has been processed in accordance with the linearised form of the Langmuir, Freundlich, Dubinin–Kaganer–Radushkevich (DKR) and Temkin isotherm equations.

The Langmuir model linearization (a plot of $1/_{qe}$ vs $1/C_e$) was expected to give a straight line with intercept of $1/q_{max}$:

$$\frac{1}{q_e} = \frac{1}{K_l q_{max}\, C_e} + \frac{1}{q_{max}} \quad (3)$$

where q_e is the amount of adsorbate adsorbed at equilibrium (mg/g) and C_e is the concentration of adsorbate in the equilibrium phase at equilibrium (ppm).

The essential characteristics of the Langmuir isotherm were expressed in terms of a dimensionless separation factor or equilibrium parameter R_L.

$$R_L = \frac{1}{1 + K_l C_o} \quad (4)$$

With C_o as initial concentration of dyes and metals in solution, the magnitude of the parameter R_L provides a measure of the type of adsorption isotherm. If $R_L > 1.0$, the isotherm is unfavourable; $R_L = 1.0$ (linear); $0 < R_L < 1.0$(favourable) and $R_L = 0$ (irreversible).

For the Freundlich isotherm the natural logarithm version was used:

$$Inq_e = InK_f + \frac{1}{n} InC_e \quad (5)$$

The DKR isotherm is reported to be more general than the Langmuir and Freundlich isotherms. It helps to determine the apparent energy of adsorption, the characteristic porosity of adsorbent toward the adsorbate and does not assume a homogenous surface or constant sorption potential.

The Dubinin–Kaganer–Radushkevich (DKR) model has the linear form

$$Inq_e = In\, X_m - \beta\varepsilon^2 \quad (6)$$

where X_m is the maximum sorption capacity, β is the activity coefficient related to mean sorption energy, and ε is the Polanyi potential, which is equal to

$$\varepsilon = RTIn\left(1 + \frac{1}{C_e}\right) \quad (7)$$

where R is the gas constant (kJ/kmol). The slope of the plot of ln q_e versus ε^2 gives β (mol^2/J^2) and the intercept yields the sorption capacity, X_m (mg/g).

The values of the adsorption energy, E, was obtained from the relationship

$$E = (2\beta)^{-1/2} \quad (8)$$

The Temkin isotherm model was also applied to the experimental data. Unlike the Langmuir and Freundlich isotherm models, this isotherm takes into account the interactions between adsorbents and metal ions to be adsorbed and is based on the assumption that the free energy of adsorption is simply a function of surface coverage. The linear form of the Temkins isotherm model equation is given in (9).

$$q_e = B\ln A + B\ln C_e \quad (9)$$

Where $B = [RT/b_T]$ in (J/mol) corresponding to the heat of adsorption, R is the ideal gas constant, T(K) is the absolute temperature, b_T is the Temkins isotherm constant and A (L/g) is the equilibrium binding constant corresponding to the maximum binding energy.

Thermodynamic Analysis

The thermodynamic parameters such as change in free energy ΔG^o, enthalpy change ΔH^o and entropy change ΔS^o were determined by using the following equations:

$$\Delta G^o = -RT\, InK_d \quad (10)$$

$$\Delta G^* = \Delta H^* - T\Delta S^* \quad (11)$$

where K_d equals the ratio of C_{solid} and C_{liquid}. C_{solid} is the equilibrium concentration of adsorbate on the adsorbent (mg/L), C_{liquid} is the equilibrium concentration of adsorbate in solution (mg/L), T is temperature (K) and R is the ideal gas constant ($8.314 J.mol^{-1}K^{-1}$).

The differential isosteric heat of adsorption (ΔH_x) at constant surface coverage was calculated using the Clausius-Clapeyron equation:

$$In\left(C_{eql}\right) = \frac{\Delta H_x}{R}\frac{1}{T} + k \quad (12)$$

where K is a constant. The differential isosteric heat of adsorption was calculated from the slope of the plot of $\ln(C_{eql})$ vs 1/T and was used for an indication of the adsorbent surface heterogeneity.

The linear form of the modified Arrhenius expression was applied to the experimental data to evaluate the activation energy (E_a) and sticking probability S* as shown in equation 13.

$$In\,(1-\theta) = S^* + \frac{E_a}{RT} \quad (13)$$

where θ is the degree of surface coverage, T is absolute solution temperature and R is gas constant ($8.314 J/mol^{-1}K^{-1}$).

Kinetic Analysis

In order to investigate the controlling mechanism of adsorption processes such as mass transfer and chemical reaction, the zero-order, first-order, second-order, third-order and pseudo-second- order equations were applied to model the kinetics of copper, lead, methylene blue and congo red adsorption onto different ratios of Mg/Al-CO_3.

Zero-order kinetic model is as shown in equation 14

$$q_t = q_e + K_o t \quad (14)$$

First-Order Kinetic model is as shown in equation 15

$$Inq_t = Inq_e + K_1 t \quad (15)$$

Second-Order Kinetic model is as shown in equation 16

$$\frac{I}{q_t} = \frac{I}{q_e} + K_2 t \quad (16)$$

Third-order kinetic model takes the form of equation 17

$$\frac{1}{q_t^2} = \frac{1}{q_e^2} + K_3 t \quad (17)$$

Pseudo-second order model takes the form of equation 18

$$\frac{t}{q_t} = \frac{1}{h_o} + \frac{1}{q_e t} \quad (18)$$

where q_e (mg/g) and q_t (mg/g) are the adsorbed amounts of dyes and metals at equilibrium and time t (min); K_o, K_1, K_2 and K_3 are the adsorption rate constants for the kinetic models.

3. Results and Discussions

Colours of Ni/Al-CO_3 crystal

The colour of the crystals is the predominant greenish colour of nickel nitrate. However, the intensity decreases with decrease in Ni/Al ratio.

Characteristics of Ni/Al-CO_3

Figures 1 and 2 show the pre-adsorption spectra of copper, lead, methylene blue and congo red and post-adsorption spectra of methylene blue and congo red on Ni/Al-LHD respectively. The strong band around 3400cm^{-1} as shown in figure 1 is associated with the stretching vibration of OH groups in the brucite like layer and interlayer molecules. The broadening of the band was attributed to the hydrogen-bond formation. Less intense absorption band around 1650 – 1500 cm^{-1} was assigned to the bending vibration of the interlayer water molecules. The carbonate ion peak is around 1400cm^{-1} which is consistent with layered double hydroxides. The sharp peaks of heterocyclic aromatic compounds are noticed between 900cm^{-1} - 700cm^{-1} in figure 2a. This is due to C-H out-of-plane vibration and is consistent with the vibration spectra of methylene blue. Figure 2b shows sharp peak around 733cm^{-1} which is characteristic of bending vibration of primary amine and phosphate bond stressing between 1100cm^{-1} - 1200cm^{-1}. This shows adsorption actually occurs via formation of complex between the congo red and the layered double hydroxides [24, 25].

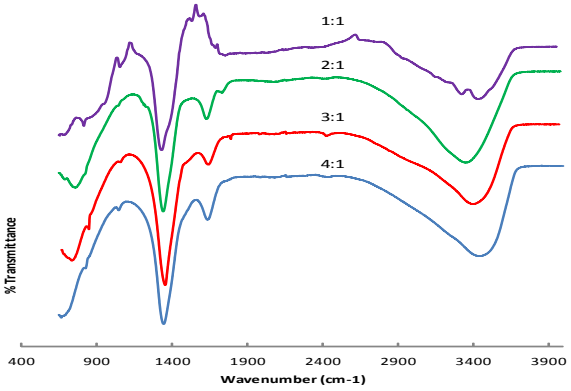

Figure 1. Pre adsorption spectra of different ratios of Ni/Al-CO_3

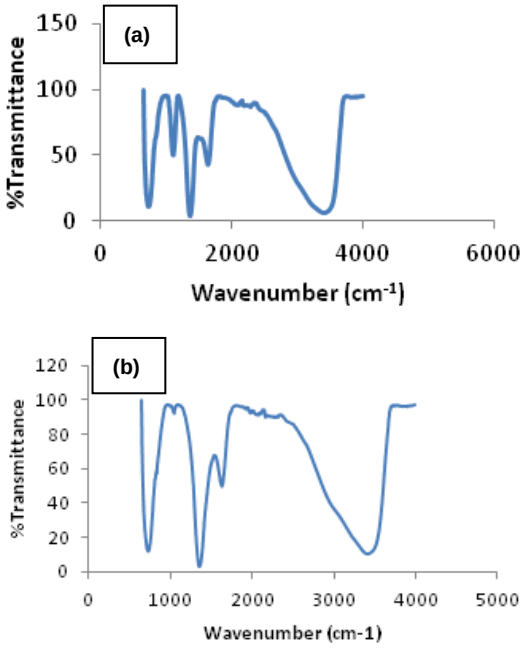

Figure 2. Ni/Al-CO_3 Fourier transform infrared spectroscopy: Post adsorption spectra of Methylene Blue (a) and Congo Reds (b)

Figures 3 and 4 show the XRD patterns of different ratios of Ni/Al-CO_3. The basal reflections are observed at low 2θ values and weaker non-basal reflections at higher 2θ. The reflections in the Ni-Al based layered double hydroxide is indexed to rhombohedral symmetry (space group R-3m). Three successive reflections at 8.5Å, 22.34Å and 34.98Å respectively, which could be indexed to (003) and (006) and (009) planes corresponding to d-spacing of 1.039nm, 0.3975nm and 0.2562nm respectively, similar to reports [26].

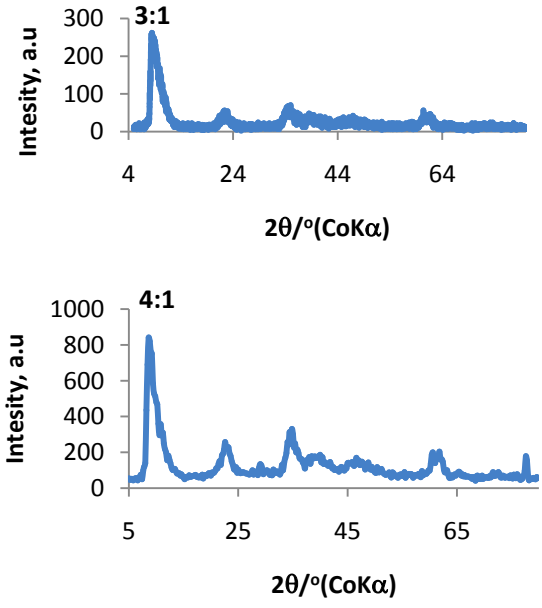

Figure 3. XRD Spectra of Ni/Al-CO_3 for Copper (3:1) and Lead (4:1) adsorption

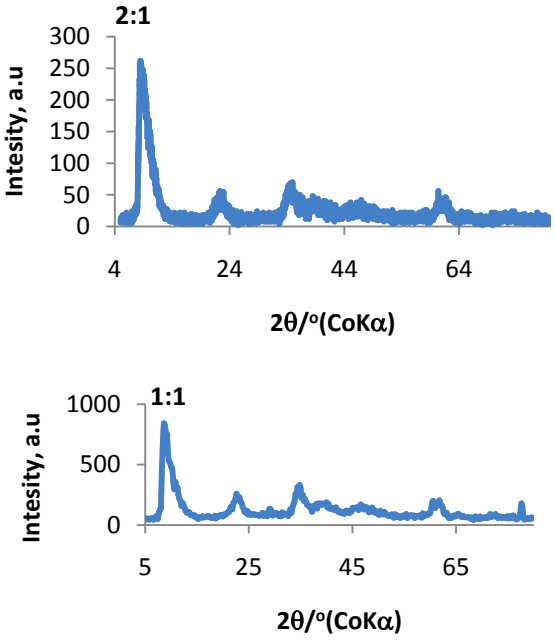

Figure 4. XRD Spectra of Ni/Al-CO_3 for Copper (2:1) and Lead (1:1) adsorption

The pre and post-adsorption SEM images and elemental analysis are shown in figures 5 - 10. The post-adsorption SEM images show coverage of available pores on the surface of the LDH while pre and post adsorption elemental analysis clearly show the adsorption of copper and lead onto the surface of the layered double hydroxides.

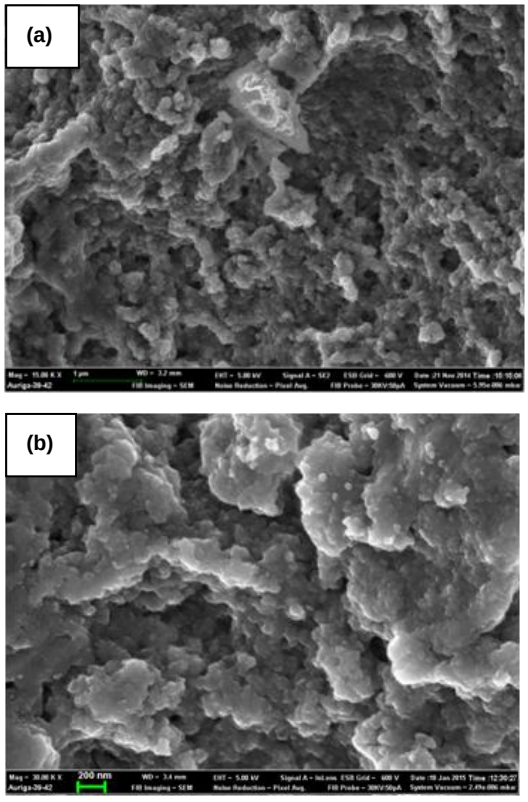

Figure 5. Scanning Electron Microscope (SEM) micrograph of Ni/Al-CO_3 before (a) and after (b) adsorption studies of Copper

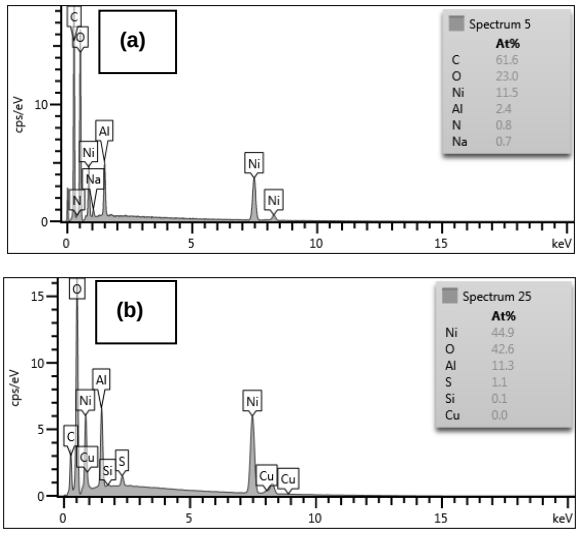

Figure 6. Energy Dispersive Spectroscopy of Ni/Al-CO_3: Pre and post Adsorption graphs indicating absence (a) and presence (b) of Copper

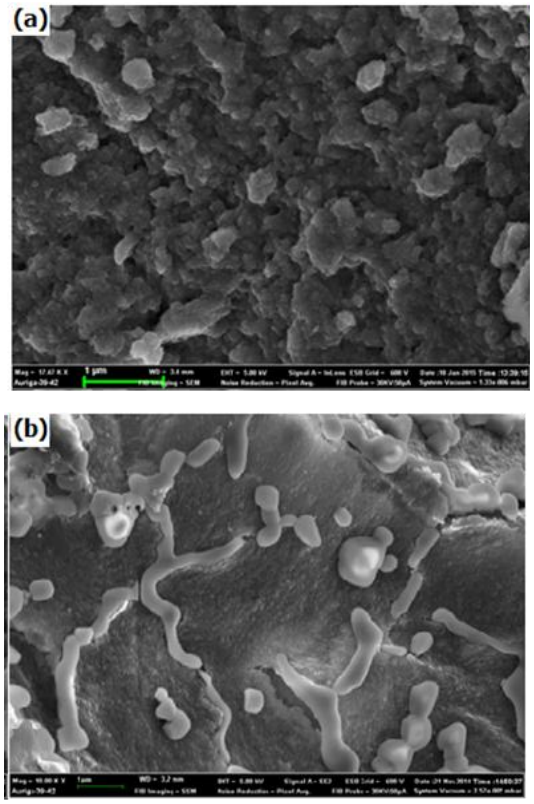

Figure 7. Scanning Electron Microscope (SEM) micrograph of Ni/Al-CO_3 before (a) and after (b) adsorption studies of Lead

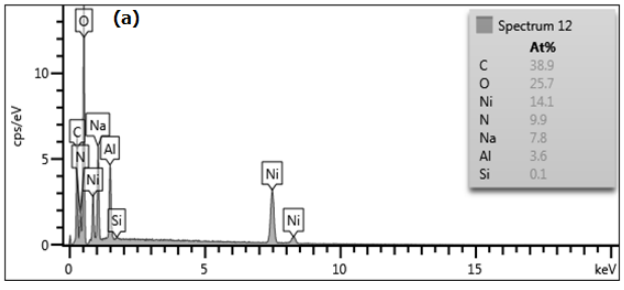

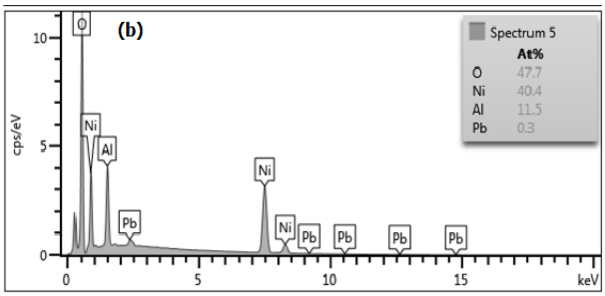

Figure 8. Energy Dispersive Spectroscopy patterns of Ni/Al-CO_3: Pre and post Adsorption graphs indicating absence (a) and presence (b) of Lead

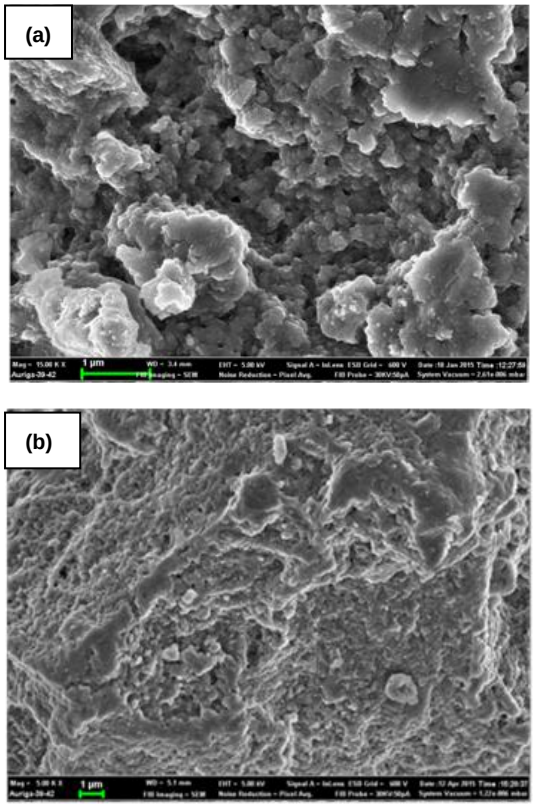

Figure 9. Scanning Electron Microscope (SEM) micrograph of Ni/Al-CO_3 before (a) and after (b) adsorption studies of Methylene Blue

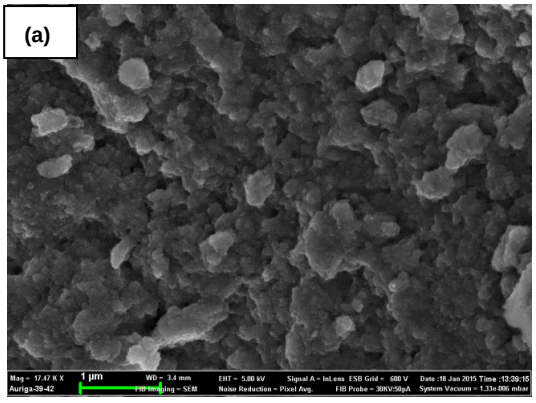

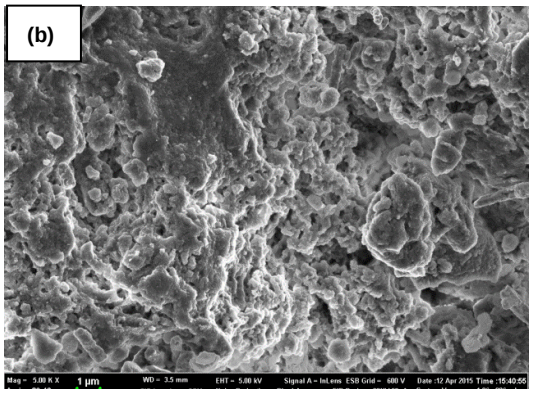

Figure 10. Scanning Electron Microscope (SEM) micrograph of Ni/Al-CO_3 before (a) and after (b) adsorption studies of Congo Red

Adsorption Studies of Ni/Al-CO_3

A good understanding of the effects of concentration, time and temperature respectively help in optimizing the process conditions for effective design purposes. Figures 11 - 14 show the plots of concentration, temperature and time in relation to removal efficiency for copper, lead, methylene blue and congo red respectively. The results indicated that the removal efficiency for metal ions and dyes increased for time and temperature respectively after equilibrium. This is due to kinetics of the molecules and increase in interaction of molecule at higher temperature.

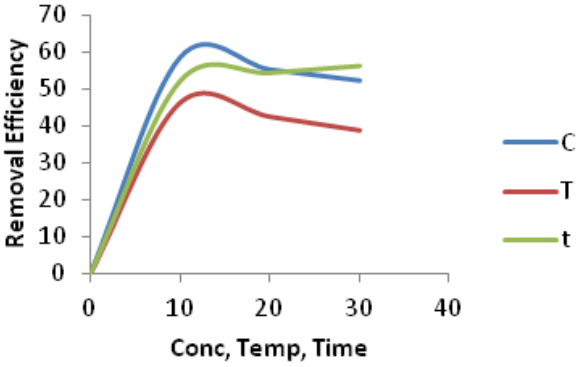

Figure 11. Effect of Concentration (C), Temperature (T) and Time (t) on the adsorption of Copper onto Ni/Al-CO_3

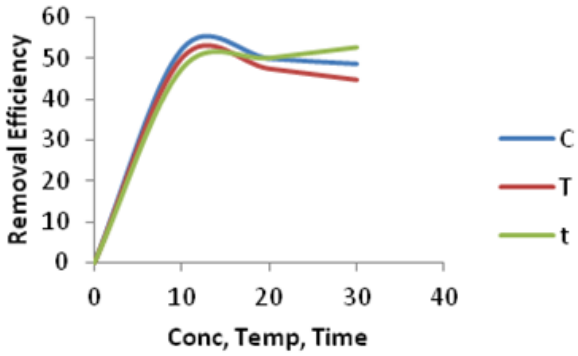

Figure 12. Effect of Concentration (C), Temperature (T) and Time (t)on the adsorption of Lead onto Ni/Al-CO_3

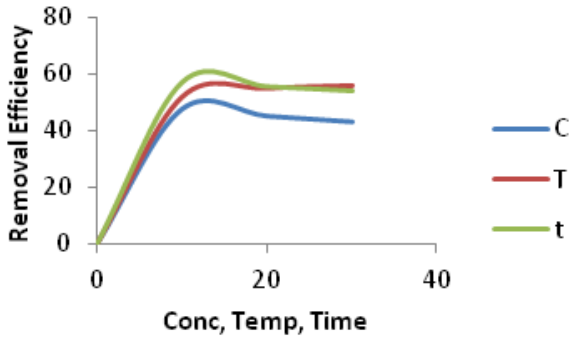

Figure 13. Effect of Concentration (C), Temperature (T) and Time (t) on the adsorption of Methylene Blue onto Ni/Al-CO_3

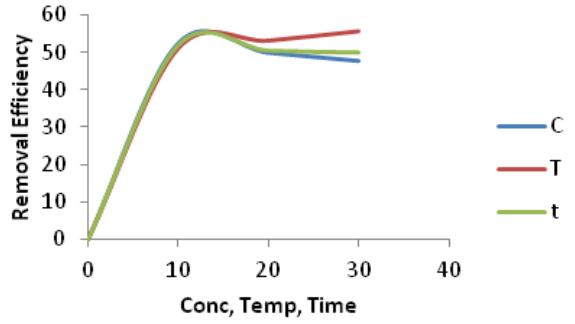

Figure 14. Effect of Concentration (C), Temperature (T) and Time (t)on the adsorption of Congo Red onto Ni/Al-CO_3

Isotherms Analysis of Ni/Al-CO_3

In this study adsorption of copper, lead, methylene blue and congo red onto different ratios of Ni/Al-CO_3 was investigated using four well-known models, the Langmuir, Freundlich, Dubinin-Kaganer-Radushkevic and Temkin isotherms.

The Langmuir constant were calculated from the linear plots of equation 3 as shown in figures 15 and 16. The influence of isotherm shape on whether adsorption is favourable or unfavourable has been considered. For a Langmuir type adsorption process, the isotherm shape can be classified by a dimensionless constant separation factor (R_L), given by equation (4). The calculated values of R_L as shown in table 1 are all within the range of 0–1, thus confirming that the uptake of copper, lead, methylene blue and congo red by the layered double hydroxide was favourable.

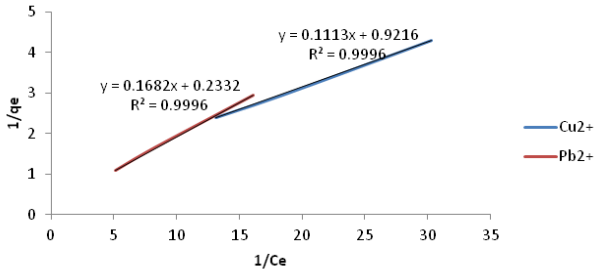

Figure 15. Langmuir Isotherm plots for adsorption of Copper and Lead onto Ni/Al-CO_3

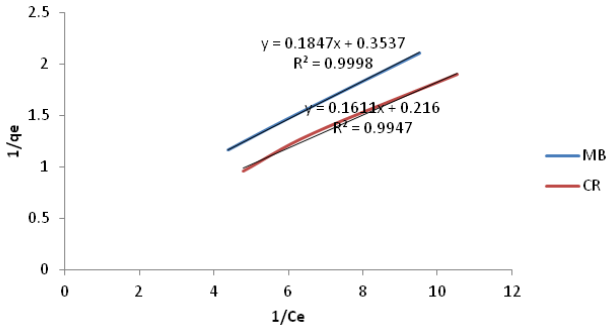

Figure 16. Langmuir Isotherm plots for adsorption of Methylene Blue and Congo Red onto Ni/Al-CO_3

From the plot of Inq_e against InC_e the Freundlich constants K_F and n which respectively indicate the adsorption capacity and the adsorption intensity, were calculated from the intercepts and slopes as shown in figures 17 and 18 and table 1 [27].

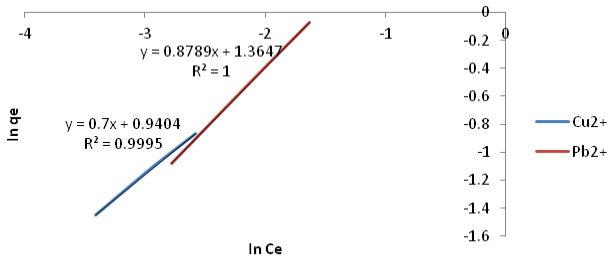

Figure 17. Freundlich Isotherm plots for adsorption of Copper and Lead onto Ni/Al-CO_3

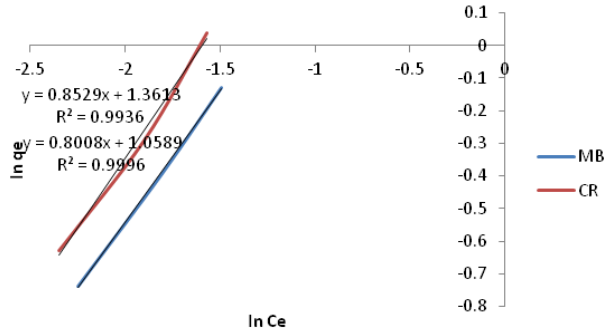

Figure 18. Freundlich Isotherm plots for adsorption of Methylene Blue and Congo Red onto Ni/Al-CO_3

The plots of lnq_e against ε^2 for copper, lead, methylene blue and congo red on different ratios of Ni/Al-CO_3 are shown in Figures 19 and 20 and the constants q_D and B_D were calculated from the intercept and slope respectively and tabulated in table 1. If the value of E lies between 8 and 16kJ/mol the sorption process is a chemisorptions one, while values of below 8kJ/mol indicate a physical adsorption process. The values E from this study shows that the adsorption mechanisms again were all physical since all figures were bellow 8KJ/mol [28, 29].

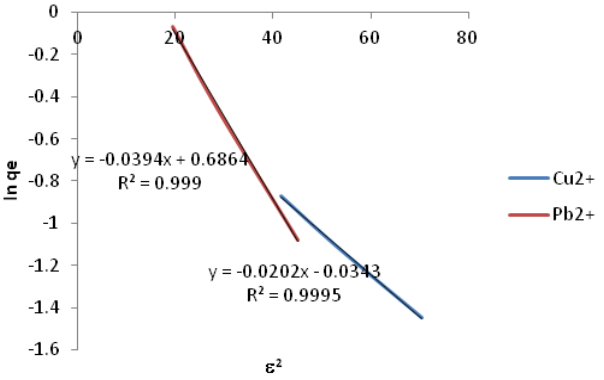

Figure 19. Dubinin-Kaganer-Radushkevic (DKR) Isotherm plots for adsorption of Copper and Lead onto Ni/Al-CO_3

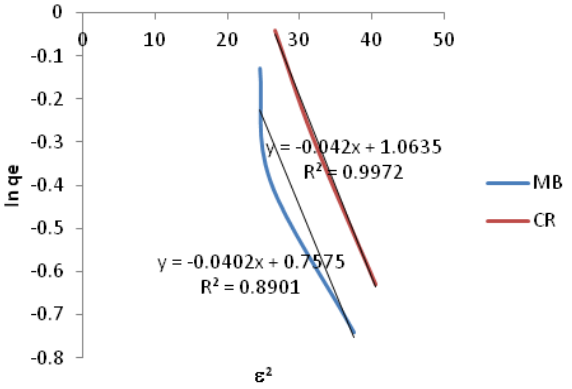

Figure 20. Dubinin-Kaganer-Radushkevic (DKR) Isotherm plots for adsorption of Methylene Blue Congo Red onto Ni/Al-CO_3

A plot of q_e versus ln C_e enables the determination of isotherm constants A and B from the slope and intercept, as shown in Figures 21 and 22. The model parameters are listed in Table 1. The adsorption energy in the Temkin model, B, is positive for copper, lead, methylene blue and congo red respectively from the aqueous solutions, which indicates that the adsorption processes were exothermic and predominantly physical.

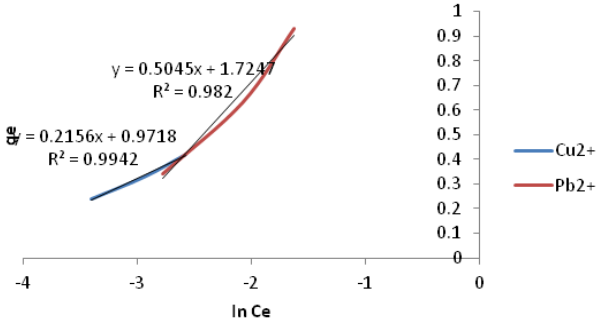

Figure 21. Temkin Isotherm plots for adsorption of Copper and Lead onto Ni/Al-CO_3

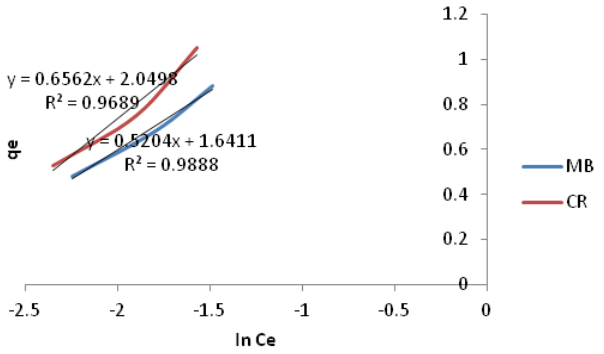

Figure 22. Temkin Isotherm plots for adsorption of Methylene Blue and Congo Red onto Ni/Al-CO_3

Table 1. Characteristic Parameters of the Adsorption Isotherm Models for Copper, Lead, Methylene Blue and Congo Red adsorption by Ni/Al-CO_3

Isotherm Model	Isotherm Parameter	Results			
		Cu^{2+}	Pb^{2+}	MB	CR
Freundlich	1/n	0.9404	1.3647	1.1473	1.1473
	K_F mg/L	2.0137	2.4082	2.1305	2.1305
	R^2	0.9995	1.0000	1.0000	1.0000
Langmuir	R_L	0.9810	0.7870	0.7000	0.7000
	R^2	0.9996	0.9996	0.9924	0.9924
Dubinin-kaganer-Radushkevich	E, KJ/mol		0.8535	0.6859	0.6859
	β_D, mol^2/KJ^2		0.6864	1.0635	1.0635
	q_D, mg/g		0.9614	0.9589	0.9589
	R^2		0.9990	0.9972	0.9972
Temkin	A mg/L	1.2484	1.3397	1.3770	1.3770
	b	$2.5x10^3$	$1.4x10^3$	$1.107x10^3$	$1.107x10^3$
	B J/mol	0.9718	1.7247	2.0498	2.0498
	R^2	0.9942	0.9820	0.9689	0.9689

Thermodynamic Studies

The values of Gibbs free energy ΔG^o, the enthalpy change (ΔH^o) and entropy change ΔS^o were calculated from equation 11 and 12 and plotted as shown in figures 23 and 24. Generally, the change in free energy from -20 to 0kJ/mol and the enthalpy up to 4.2kJ/mol are characteristic of physical adsorption (due to relatively weak van der Waals attraction forces), whereas the change in free energy between -80 and -40kJ/mol and enthalpy more than 21kJ/mol indicate chemical adsorption (due to stronger interactions involving ionic or covalent bonding sorbate-sorbent) [30, 31]. A positive ΔH^o suggests that sorption proceeded favourably at higher temperature and the sorption mechanism was endothermic for the dyes. A positive value of ΔS^o reflects the affinity of the adsorbent towards the adsorbate species. The adsorption of metal ions is a direct opposite of the dyes, the process was exothermic and proceeded favourably at lower temperatures. In addition, positive value of ΔS^o suggests increased randomness at the solid/solution interface with some structural changes in the adsorbate and the adsorbent. The results in table 2 indicate that the relatively low/negative ΔG^o values are consistent with spontaneous adsorption process. The negative ΔH^o values for metal ions and the positive ΔH^o values confirms that the adsorption of metal ions was exothermic and proceeded favourably at low temperature while that of dyes is endothermic and maximized at high temperature.

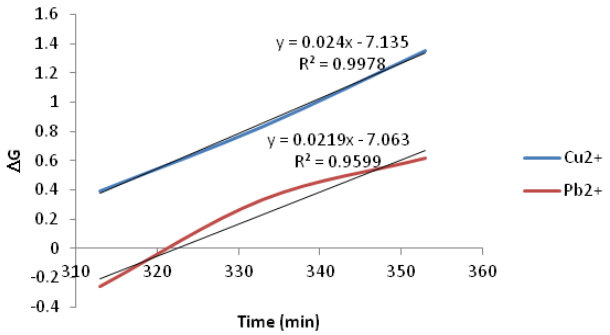

Figure 23. Plots of ΔG^o vs. Temperature for the adsorption of Copper and Lead onto Ni/Al-CO_3

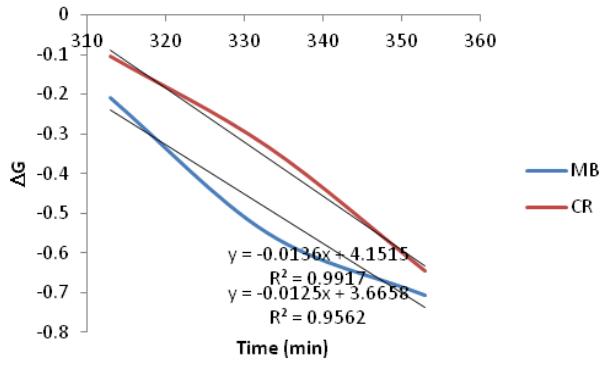

Figure 24. Plots of ΔG^o vs. Temperature for the adsorption of Methylene Blue and Congo Red onto Ni/Al-CO_3

Isosteric heat of adsorption ΔH_x is the energy difference before and after adsorption and understanding it would help in optimizing the design and surface dynamics of the process. The plots of InC_e against 1/T in figures 25 and 26 gave slopes equal to ΔH_x (table 2). The magnitude of ΔH_x gives information about the adsorption mechanism as chemical, ion-exchange or physical sorption. For physical adsorption, ΔH_x should be below 80kJ mol^{-1} and for chemical adsorption it ranges between 80 and 400kJ mol^{-1}. The ΔH_x values in this study show the adsorption process is physical [32, 33].

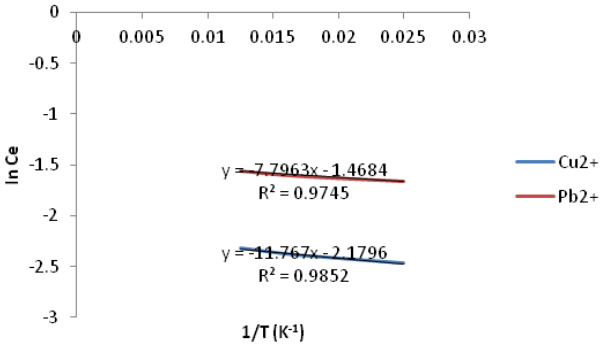

Figure 25. Plots of In C_e vs. 1/T for the adsorption of Copper and Lead Red onto Ni/Al-CO_3

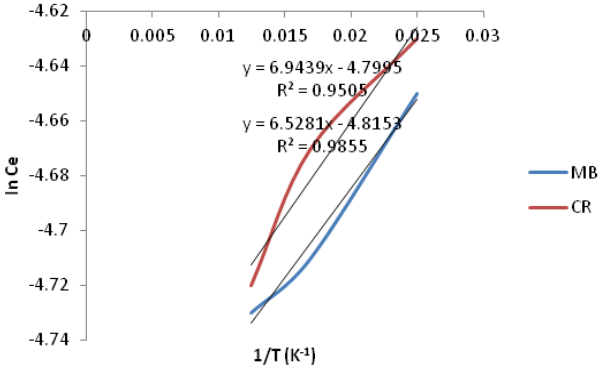

Figure 26. Plots of In C_e vs. 1/T for the adsorption of Methylene Blue & Congo Red onto Ni/Al-CO_3

The plots of In (1-θ) versus 1/t using equation 13 yielded straight lines as presented in figures 27 and 28. The activation energies E_a and sticking probability S* were calculated from the slopes and intercepts, respectively. The values of E_a and S* were shown in table 2. The relatively low and negative E_a values indicate that low temperature or energy favours metal adsorption while higher temperature favours dye adsorption. Relatively low values of E_a also suggest that the sorption processes were diffusion controlled. The sticking probability S* indicates the measure of the potential of an adsorbate to remain on the adsorbent. It is often interpreted as S*>1 (no sorption), S*=1 (mixture of physic-sorption and chemisorption), S* = 0 (indefinite sticking – chemisorption), 0<S*<1 (favourable sticking – physic- sorption). Again the values of S* obtained here indicate physical adsorption.

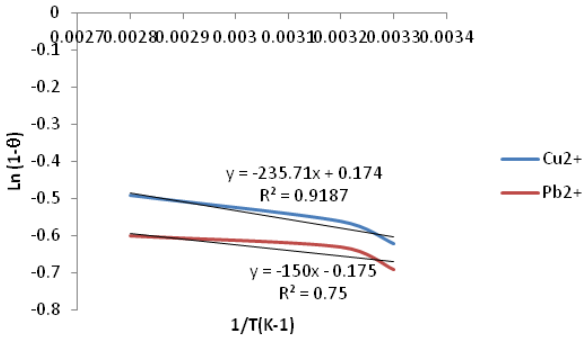

Figure 27. Plots of Ln(1-θ) vs. 1/T(K^{-1}) for the adsorption of Copper and Lead Ni/Al-CO_3

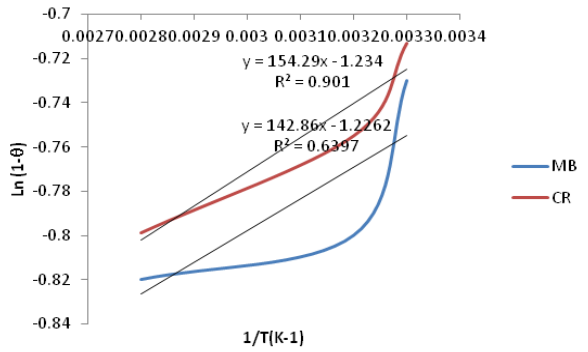

Figure 28. Plots of Ln(1-θ) vs. 1/T(K^{-1}) for the adsorption of Methylene Blue and Congo Red onto Ni/Al-CO_3

Table 2. Thermodynamic Parameters of the Adsorption of Copper, Lead, Methylene Blue and Congo Red onto Ni/Al-CO_3

T, K	ΔG°, KJ/mol	ΔH°, KJ/mol	ΔS°, J/molK	Ea KJ/mol	ΔHx KJ/mol	S*
Copper						
313	0.390	-7.135	24.0	1.447	18.1	0.45
333	0.831					
353	1.350					
Lead						
313	-0.260	-7.063	21.9	-1.45	12.21	0.48
333	0.333					
353	0.616					
Methylene Blue						
313	-0.550	3.6658	12.5	-10.19	40.03	0.48
333	-0.550					
353	-0.707					
Congo Red						
313	-0.104	4.1515	13.5	-9.34	39.9	0.49
333	-0.332					
353	-0.646					

Kinetic Studies of Ni/Al-CO_3

The adsorption kinetic study is important in predicting the mechanism (chemical reaction or mass-transport process) that control the rate of the pollutant removal and retention time of adsorbed species at the solid-liquid interface. The results of R^2 in table 3 shows that lead, methylene and congo red adsorption onto different ratios of Ni/Al-CO_3 fitted the different kinetic models, whereas pseudo-second-order kinetic model best interpret the adsorption of copper.

Table 3. Correlation coefficient values of Copper, Lead, Methylene Blue and Congo Red for different kinetic orders (Ni/Al-CO_3)

Kinetic Orders	Copper R^2	Lead R^2	Methylene Blue R^2	Congo Red R^2
Zero-Order	0.1378	1	0.9643	1
First-Order	0.1071	0.9973	0.9643	0.9998
Second-Order	0.1071	0.9973	0.9614	0.9999
Pseudo-Second Order	0.9466	0.9991	0.9994	0.9999
Third-Order	0.0913	0.9994	0.9566	0.9997

4. Conclusions

It can be concluded that Ni/Al-CO_3 can be employed as adsorbent for the removal of Lead (II), copper (II), methylene blue (MB) and congo red (CR) from aqueous solutions. However, contact time, temperature and initial concentration of dyes and metals could either affect the adsorption capacities of the layered double hydroxide positively or negatively depending on the range of the parameters. The application of the experimental data in defining equilibrium and thermodynamic parameters is consistent with physical adsorption. This indicates that Ni/Al-layered double hydroxide is indeed a novel adsorbent.

REFERENCES

[1] Jha, S., Dikshit S.N., AND Pandey, G. Comparative studies of bacteria and fungi for the removal of cu2+ metal. International Journal of Pharma and Bio Sciences, 2, pp. 133-139. 2011.

[2] Ayawei, N., Angaye, S.S., Wankasi, D. and Dikio, E.D. (2015) Synthesis, Characterization and Applica- tion of Mg/Al Layered Double Hydroxide for the Degradation of Congo Red in Aqueous Solution. Open Journal of Physical Chemistry, 5, 56-70.

[3] Ngah, W.S.N. and Hanafiah, M.A.K.M. Removal of heavy metal ions from waste water by chemically modified plant waste as adsorbents. Bioresource Technology 99 pp.3935–3948. 2008.

[4] Qiuhong Hu, Zhiping Xu, Shizhang Qiao, Fouad Haghseresht, Michael Wilson, Gao Qing Lu, et al, A novel color removal adsorbent from heterocoagulation of cationic and anionic clays. Journal of Colloid and Interface Science. 308 (1): p. 191-199. 2007.

[5] L. S. Oliveira, A. S. Franca, T. M. Alves, S. D. F. Rocha "Evaluation of untreated coffee husks as potential biosorbents for treatment of dye contaminated waters," J. Hazard. Mater., vol. 155, pp. 507-512. 2008.

[6] Ayhan demirbas. Heavy metal adsorption onto agro-based

waste materials: a review. Journal. Haza. mater. 157, 220 – 229. 2008.

[7] Han, R., Zhang, J., Zou, W., Shi, J., Liu, H., Treatment of liquid effluents from Hot dip galvanization by the couple lime/chitosan J. Harz. Mater. 125, 266. 2005.

[8] Ho, Y.S., Chiu, W.T. and Wang, C.C, Regression analysis for the sorption isotherms of basic dyes on sugarcane dust. *Bioresource Technology*, 96 (11), 1285-1291. 2005.

[9] Sagar, R., Kumar, B., Dumka, U.C., Krishna Moorthy, K. and Pant, P. (2004). Characteristics of aerosol spectral optical depths over Manora Peak: A high-altitude station in the central Himalayas. Journal of Geophysical Research. Atmospheres 109.

[10] Ho, Y. S. Second-order kinetic model for the sorption of cadmium onto tree fern: a comparison of linear and non-linear methods.Water Res. 40, 119. 2006.

[11] V.K. Gupta, I. Ali, Suhas, D. Mohan, Equibrium uptake and sorption dynamics for the removal of a basic dye using low-cost adsorbents, J. Coll. Interface Sci. 265, 257-264. 2003.

[12] Santhi, T., Manonmani, S., Smitha T., Chem. Eng. Res. Bull., 14, 11. 2010.

[13] Malana, M. A., Ijaz, S., Ashiq, N. Removal of various dyes from aqueous media onto polymeric gels by adsorption process: Their kinetics and thermodynamics Desalination, 263 249. 2010.

[14] Wang L.G., Yan, G.B. Adsorptive removal of direct yellow 161 dye from aqueous solution using bamboo charcoals activated with different chemicals Desalination, 274, 81, 2011.

[15] Choy, J.H., Kim, Y.K., Son, Y.H., Choy, Y.B., Oh, J.M., Jung, H., & Hwang, S.J. Nanohybrids of edible dyes intercalated in ZnAl layered double hydroxides, Journal of Physics and Chemistry of Solids, 69, 1547– 1551, 2008.

[16] Marangoni, R., Bouhent, M., Gueho, C.T., Wypych, F., & Leroux, F. Zn2Al layered double hydroxides inter- calated and adsorbed with anionic blue dyes: A physico- chemical characterization, Journal of Colloid and Inter- face Science, 333, 120–127, 2009.

[17] Zhang, P., Qian, G., Shi, H., Ruan, X., Yang, J., & Frost, R.L. Mechanism of interaction of hydrocalumites (Ca/Al-LDH) with methyl orange and acidic scarlet GR, Journal of Colloid and Interface Science, 365, 110–116, 2012.

[18] Bouhent, M.M., Derriche, Z., Denoyel, R., Prevot, V., & Forano, C. Thermodynamical and structural insights of orange II adsorption by MgRAlNO3 layered double hydroxides, Journal of Solid State Chemistry, 184, 1016–1024, 2011.

[19] F. Kovanda, E. Jindov´a, K. Lang, P. Kub´at, and Z. Sedl´akov´a "Preparation of layered double hydroxides intercalated with organic anions and their application in LDH/poly (butyl methacrylate) nanocomposites," Applied Clay Science, vol. 48, no. 1, pp. 260–270, 2010.

[20] F. Cavani, F. Trifir`o, and A. Vaccari. "Hydrotalcite-type anionic clays: preparation, properties and applications," Catalysis Today, vol. 11, no. 2, pp. 173–301, 1991.

[21] Ayawei, N. Inengite A. K., Ekubo A. T., Wankasi, D. and Dikio, E. D. Mg/Fe layered double hydroxide for removal of lead (ii): Thermodynamic, equilibrium and kinetic studies. European Journal of Science and Engineering, 3 (1), 1-17, 2015.

[22] El Mouloudi Sabbar, Marie Elisabeth de Roy, Fabrice Leroux. Probing the interaction between di- and tri-functionalized carboxy- phosphonique acid and LDH layer structure.Journal of Physics and Chemistry of Solids 67, 2419-2429, 2006.

[23] N. Sadik, E. Sabbar, M. Mountadar Elimination of the pesticides by synthesized anion clays starting from marine water. J. Mater. Environ. Sci. 3 (2), 379-390, 2012.

[24] Chongrak, K., Eric, H., Noureddine A. and Jean P. G., "Application of Methylene Blue Adsorption to Cotton Fiber Specific Surface Area Measurement: Part I. Methodology", The Journal of Cotton Science 2: 164 - 173, 1998.

[25] S. Mariam Sumari, Yamin Yasin and Zaini Hamzah, "Adsorption of Anionic Amido Black Dye by Layered Double Hydroxide, $ZnAlCO_3$-LDH" Malaysian Journal of Analytical Sciences, vol. 13, pp. 120 -128, 2009.

[26] Yi Liu, Tongwen Yu, Rui Cai, Yanshuo Li, Weishen Yang and Jurgen Caro, "One-Pot Synthesis of NiAl-CO_3 LDH Anti-Corrosion Coatings from CO_2-Saturated Precursors", Electronic Supplementary Material (ESI) for RSC Advances, 2015.

[27] Ayawei N., Ekubo A. T., Wankasi D., & Dikio E. D. Synthesis and Application of Layered Double Hydroxide for the removal of Copper in Wastewater. International Journal of Chemistry; Vol. 7, No. 1; 2015.

[28] Dada, A. O., Olalekan, A. P., Olatunya, A. M. and Dada, O. "Langmuir, Freundlich, Temkin and Dubinin-Radushkevich Isotherms Studies of Equilibrium Sorption of Zn^{2+} Unto Phosphoric Acid Modified Rice Husk" Journal of Applied Chemistry, vol. 3, pp. 38 - 45, 2012.

[29] Flavio, A. P., Silvio L. P. D., Ede, C. L., Edilson, V. B., "Removal of Congo red from aqueous solution by anilinepropylsilica xerogel", Dyes and Pigments, Vol. 76, pp 64 - 69, 2008.

[30] Horsfall, M.; Spiff, A. I. and Abia, A. A. Studies on the influence of mercaptoacetic acid (MAA) modification of cassava (Manihot sculenta cranz). waste biomass on the adsorption of Cu^{2+} and Cd^{2+} from aqueous solution. Bull. Korean Chem. Soc., 25(7), 969-976, 2004.

[31] P. Senthil Kumar, K. Kirthika. "Equilibrium And Kinetic Study Of Adsorption Of Nickel From Aqueous Solution Onto Bael Tree Leaf Powder" Journal of Engineering Science and Technology, vol. 4, pp. 351 - 363, 2009.

[32] Papita Saha and Shamik Chowdhury. "Insight into Adsorption Thermodynamics", InTech, ISBN:978-953-307-544-0, Vienna, Austria, 2011.

[33] Svetlana Lyubchik, Andrey Lyubchik, Olena Lygina, Sergiy Lyubchik and Isabel Fonseca. Comparison of the Thermodynamic Parameters Estimation for the Adsorption Process of the Metals from Liquid Phase on Activated Carbons, ISBN: 978-953-307-563-1, InTech Caparica Portugal, 2011.